Title

High-Spatial-Resolution Multishot Multiplexed Sensitivity-encoding Diffusion-weighted Imaging for Improved Quality of Breast Images and Differentiation of Breast Lesions: A Feasibility Study.

Journal

Radiology: Imaging Cancer, 2(3)

Authors

Larowin, Toni
Fung, Maggie
Guidon, Arnaud
et al.

Publication Date

2020-05-01

DOI

10.1148/rycan.2020190076

Peer reviewed

Radiology: Imaging Cancer

TECHNICAL DEVELOPMENT

High-Spatial-Resolution Multishot Multiplexed Sensitivity-encoding Diffusion-weighted Imaging for Improved Quality of Breast Images and Differentiation of Breast Lesions: A Feasibility Study

Isaac Daimiel Naranjo, MD • Roberto Lo Gullo, MD • Elizabeth A. Morris, MD • Toni Larowin, BS • Maggie M. Fung, MS • Arnaud Guidon, PhD • Katja Pinker, MD, PhD • Sunitha B. Thakur, MSc, PhD

From the Department of Radiology, Breast Imaging Service, Memorial Sloan Kettering Cancer Center, New York, NY (I.D.N., R.L.G., E.A.M., T.L., K.P., S.B.T.); Department of Radiology, Breast Imaging Division, Istituto Europeo di Oncologia, Milan, Italy (R.L.G.); MR Application and Workflow Team, GE Healthcare, New York, NY (M.M.F.); MR Application and Workflow Team, GE Healthcare, Boston, Mass (A.G.); Department of Biomedical Imaging and Image-guided Therapy, Molecular and Gender Imaging Service, Medical University of Vienna, Vienna, Austria (K.P.); and Department of Medical Physics, Memorial Sloan Kettering Cancer Center, 1275 York Ave, New York, NY 10065 (S.B.T.). Received September 18, 2019; revision requested November 21; revision received December 19; accepted January 23, 2020. **Address correspondence to** S.B.T. (e-mail: *thakurs@mskcc.org*).

Conflicts of interest are listed at the end of this article.

Radiology: Imaging Cancer 2020; 2(3):e190076 • https://doi.org/10.1148/rycan.2020190076 • Content codes: BR OI

Purpose: To compare multiplexed sensitivity-encoding (MUSE) diffusion-weighted imaging (DWI) and single-shot DWI for lesion visibility and differentiation of malignant and benign lesions within the breast.

Materials and Methods: In this prospective institutional review board–approved study, both MUSE DWI and single-shot DWI sequences were first optimized in breast phantoms and then performed in a group of patients. Thirty women (mean age, 51.1 years ± 10.1 [standard deviation]; age range, 27–70 years) with 37 lesions were included in this study and underwent scanning using both techniques. Visual qualitative analysis of diffusion-weighted images was accomplished by two independent readers; images were assessed for lesion visibility, adequate fat suppression, and the presence of artifacts. Quantitative analysis was performed by calculating apparent diffusion coefficient (ADC) values and image quality parameters (signal-to-noise ratio [SNR] for lesions and fibroglandular tissue; contrast-to-noise ratio) by manually drawing regions of interest within the phantoms and breast tumor tissue. Interreader variability was determined using the Cohen κ coefficient, and quantitative differences between MUSE DWI and single-shot DWI were assessed using the Mann-Whitney *U* test; significance was defined at $P < .05$.

Results: MUSE DWI yielded significantly improved image quality compared with single-shot DWI in phantoms (SNR, $P = .001$) and participants (lesion SNR, $P = .009$; fibroglandular tissue SNR, $P = .05$; contrast-to-noise ratio, $P = .008$). MUSE DWI ADC values showed a significant difference between malignant and benign lesions ($P < .001$). No significant differences were found between MUSE DWI and single-shot DWI in the mean, maximum, and minimum ADC values ($P = .96$, $P = .28$, and $P = .49$, respectively). Visual qualitative analysis resulted in better lesion visibility for MUSE DWI over single-shot DWI (κ = 0.70).

Conclusion: MUSE DWI is a promising high-spatial-resolution technique that may enhance breast MRI protocols without the need for contrast material administration in breast screening.

Supplemental material is available for this article.

Diffusion-weighted imaging (DWI) is increasingly used for breast tumor detection and characterization in clinical practice (1), with single-shot DWI echo-planar imaging routinely used as the main DWI sequence. However, single-shot DWI lacks high spatial resolution and is sensitive to patient motion and magnetic field inhomogeneities, which leads to imaging artifacts (eg, distortion, ghosting, aliasing), often preventing adequate delineation of small lesions (1,2).

Multishot DWI echo-planar imaging techniques offer higher spatial resolution but are susceptible to motion-induced phase errors since each individual shot may have a different diffusion-encoding direction. This results in ghosting artifacts, pixel misregistration, and low image resolution with poor diffusion contrast on the reconstructed images (3). Moreover, apparent diffusion coefficient (ADC) values may be altered, yielding inexact measures that may affect diagnosis (4). Techniques such as interleaved echo-planar imaging (5) or periodically rotated overlapping parallel lines with enhanced reconstruction (known as PROPELLER) (6,7) have been introduced to reduce geometric distortion in multishot DWI; however, they require prolonged scan times that limit their clinical applicability (8).

Navigator-based acquisition may be useful to prevent artifacts by estimating phase-encoding variations between interleaves, but motion can occur between the interleaf and navigator acquisition, restricting clinical applicability (9,10). While phase correction strategies without the use of navigator echoes have also been investigated with iterative computational algorithms (11), these may not be sufficient to resolve nonlinear phase errors resulting from local motion in

Abbreviations

ADC = apparent diffusion coefficient, CNR = contrast-to-noise ratio, DWI = diffusion-weighted imaging, MUSE = multiplexed sensitivity encoding, SNR = signal-to-noise ratio

Summary

Multishot multiplexed sensitivity-encoding diffusion-weighted imaging is a feasible and easily implementable routine breast MRI protocol that yields high-quality diffusion-weighted breast images.

Key Points

- Multishot multiplexed sensitivity-encoding (MUSE) diffusion-weighted imaging (DWI) for breast tumors is a feasible technique that yields high-quality breast diffusion-weighted images and outperforms single-shot DWI for artifact correction and quality of breast images.
- Mean, maximum, and minimum apparent diffusion coefficient values from MUSE DWI and single-shot DWI were comparable, with no significant differences ($P = .96$, $P = .28$, and $P = .49$, respectively).
- Apparent diffusion coefficient values calculated from MUSE DWI were significantly lower in malignant lesions than in benign breast lesions ($P < .001$).

multishot DWI. Reconstruction strategies without phase estimation may be helpful, such as through using locally low-rank regularization to amend shot-to-shot phase mismatches (12).

One of the most promising techniques to amend motion-induced phase errors is multiplexed sensitivity-encoding (MUSE) diffusion-weighted imaging (DWI) (13). MUSE DWI integrates a sensitivity-encoding (14) parallel imaging method and achieves a better signal-to-noise ratio (SNR) given its improved matrix inversion conditioning. MUSE DWI may reduce ghosting artifacts and geometric distortions, enabling acquisition of high-spatial-resolution images within a clinically feasible acquisition time and alleviating the need for navigator echoes or any pulse sequence modification.

The aim of our study was to optimize MUSE DWI using breast phantoms to achieve the highest spatial resolution with minimal artifacts compared with single-shot DWI, evaluate the feasibility of optimized MUSE DWI in patients for breast lesion detection, and qualitatively and quantitatively compare MUSE DWI with single-shot DWI. We show through multiple analyses that MUSE DWI sequences provide optimal imaging resolution and quality over single-shot DWI and have differential ADC values for malignant and benign lesions. Together, our results suggest that MUSE DWI could be translated into a routine breast MRI protocol yielding high-quality images and enhanced detection of malignant lesions.

Table 1: Clinicopathologic Characteristics of 37 Breast Lesions in 30 Women

Characteristic	Value
Age (y)	
Mean	51.1 ± 10.1
Median	52
Range	27–70
Menopausal status (30 patients)	
Premenopausal	12 (40)
Postmenopausal	18 (60)
Standard of reference for lesions (37 lesions)	
Histopathology	31 (83.7)
Follow-up (≥2 years)	3 (8.1)
None	3 (8.1)
Benign lesions (15 lesions)	
Fibroadenoma	2 (13.3)
Papilloma	1 (6.7)
Sclerosing adenosis	3 (20)
Benign breast parenchyma	5 (33.3)
Fibromatosis	1 (6.7)
Stable lesions in follow-up	3 (20)
Malignant lesions (19 lesions)	
IDC	17 (89.5)
IDC with DCIS	2 (10.5)
Subgroup of 22 participants with 28 lesions with confirmed disease or follow-up for lesion differentiation	
Malignant lesions (15 lesions)	
IDC	13 (86.7)
IDC with DCIS	2 (13.3)
Benign lesions (13 lesions)	
Fibroadenoma	1 (7.7)
Papilloma	1 (7,7)
Sclerosing adenosis	3 (23.1)
Benign breast parenchyma	4 (30.8)
Fibromatosis	1 (7.7)
Stable lesions in follow-up	3 (23.1)

Note.—Unless stated otherwise, data in parentheses are percentages. Percentages may not add up to 100 because of rounding. DCIS = ductal carcinoma in situ, IDC = invasive ductal carcinoma.

Materials and Methods

Study Design

This prospective study was approved by an institutional review board at Memorial Sloan Kettering Cancer Center and was conducted in compliance with the Health Insurance Portability and Accountability Act. From March to May 2019, 72 women underwent MUSE DWI protocol D (two shots; acceleration factor, two) after a full breast MRI diagnostic protocol. Technical details are shown in Table E1 (supplement). All women provided written informed consent. There was no participant overlap with other studies. For this project, of the 72 women, 30 (mean age, 51.1 years ± 10.1[standard deviation]; age range, 27–70 years) with a total of 37 solid mass lesions (mean size, 15.4 mm ± 13; size range, 5–56 mm) categorized as Breast Imaging Reporting and Data System (BI-RADS) category 2 to 5 at dynamic contrast material–enhanced MRI were included for lesion visibility

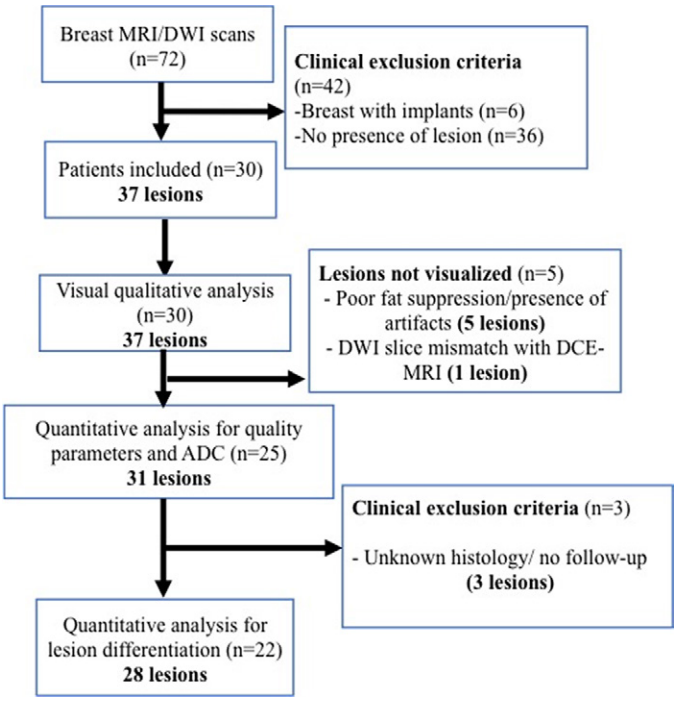

Figure 1: Flowchart for patient selection. ADC = apparent diffusion coefficient, DCE-MRI = dynamic contrast-enhanced MRI, DWI = diffusion-weighted image, *n* = number of patients.

and qualitative assessment. Histologic findings revealed 15 benign lesions and 19 invasive ductal carcinomas, of which two had associated ductal carcinoma in situ. The average lesion size was 9.4 mm ± 4 (range, 5–21 mm) for benign lesions and 21.6 mm ± 15 (range, 6–56 mm) for malignant lesions. Three lesions lacked either histologic findings or follow-up data. Participant characteristics and tumor histopathologic features are summarized in Table 1.

After qualitative assessment, six lesions were not visible on diffusion-weighted images, resulting in a total of 31 lesions used for the quantitative comparison of single-shot DWI and MUSE DWI (Fig 1). The three lesions without histologic findings or follow-up were not eligible for lesion differentiation; thus, they were excluded, resulting in 28 lesions (15 malignant, 13 benign) in 22 participants.

Twenty-five lesions were biopsied, and only three lesions were classified as BI-RADS category 2 at MRI after remaining unchanged at follow-up (≥2 years).

MRI Examinations

All MRI examinations were performed using a 3-T system (Discovery MR750; GE Healthcare, Milwaukee, Wis) with a dedicated 16-channel phased-array breast coil (Vanguard, Sentinelle Medical, Toronto, Ontario, Canada) as the receiver. Parameters for DWI sequences are found in Table E2 (supplement).

Technical Descriptions

MUSE pulse sequence.—Conventional single-shot DWI collects all the data for a single slice in one shot. When a higher matrix size is desired to maintain resolution over a large coverage, as in breast imaging, phase errors accumulate, resulting in spatial encoding inconsistencies that lead to distortion. MUSE splits the single-shot echo-planar imaging acquisition into multiple shots to reduce this distortion at the expense of increased scan time. The MUSE k-space trajectory is generated by starting with the k-space pattern needed for an accelerated single-shot DWI undersampled in the phase-encoding direction. The pattern is then successively shifted along the phase-encoding direction for subsequent shots. As shown in Figure E1 (supplement), which illustrates a four-shot acquisition, the k-space trajectory for the first shot is identical to single-shot DWI with an acceleration factor of four.

MUSE reconstruction algorithm.—MUSE reconstruction is intended to mitigate random shot-to-shot phase errors that arise from patient motion occurring while the diffusion-sensitizing gradients are turned on. As such, the algorithm proceeds in two steps (Fig E2 [supplement]). First, phase maps are estimated for each shot using a parallel imaging reconstruction method (eg, array coil spatial sensitivity encoding) (15). The phase maps from all shots are then combined with the coil sensitivities obtained during a routine calibration scan to create pseudo sensitivities, as illustrated. In the second step, a pseudo sensitivity inverse matrix is computed, and the final images are created by solving for the unaliased images.

MUSE DWI Protocol Optimization on Breast Phantoms

MUSE DWI was first optimized using breast phantoms (Quantitative Imaging Biomarkers Alliance breast phantom model 131; High Precision Devices, Boulder, Colo). DWI was performed, consisting of one axial two-dimensional single-shot DWI acquisition followed by six two-dimensional MUSE DWI acquisitions (protocols A–F) (Table E1 [supplement]). Phantom studies were repeated six times across different days to enable repeatability and reproducibility assessment. All phantom images were visually evaluated. Two radiologists (I.D.N. and K.P., with 4 and 14 years of experience) assessed the images for overall image quality and the presence of artifacts.

Readers (I.D.N. and R.L.G., each with 4 years of experience) chose the optimal protocol (yielding the best image quality within clinically acceptable scan times) for the participant study in consensus. ADC parametric maps were calculated for both sequences using two *b* values (0 and 800 sec/mm^2) using the READY View application on the Advantage Workstation (GE Healthcare, Milwaukee, Wis). SNR values were calculated using OsiriX software (version 6.0; OsiriX Foundation, Geneva, Switzerland) according to the literature (16). Quantitative parameters were compared between MUSE DWI and single-shot DWI.

Qualitative comparison assessment of single-shot DWI and MUSE DWI.—Two breast imaging radiologists (I.D.N. and R.G.L., each with 4 years of experience) evaluated the images independently while being blinded to the clinical diagnosis.

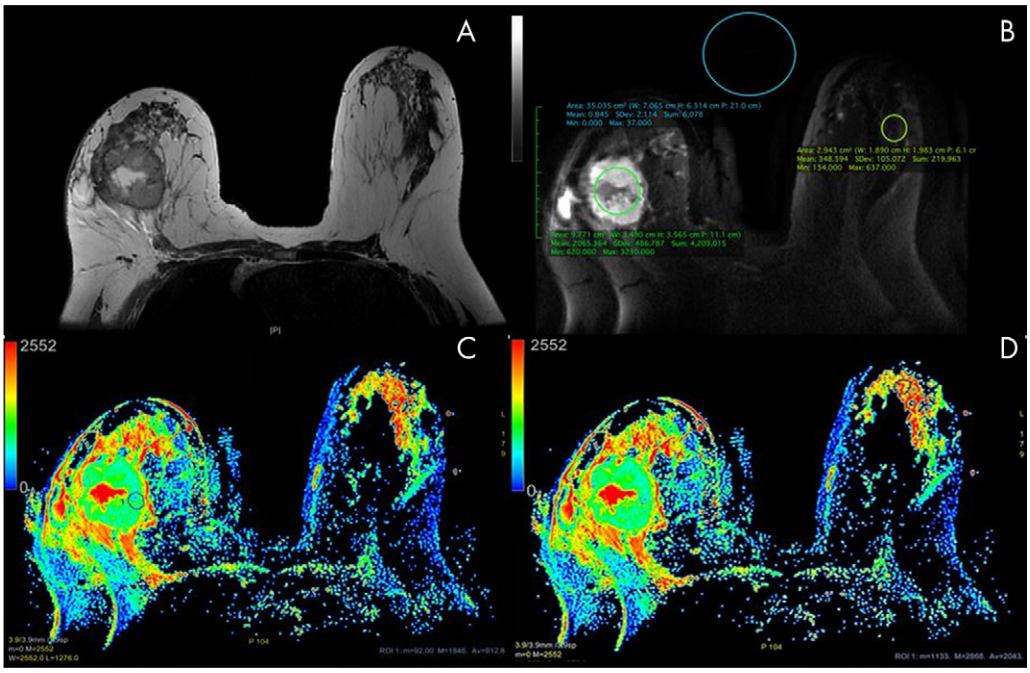

Figure 2: Axial images in a 59-year-old woman with a 50-mm invasive ductal carcinoma in the right breast. *A*, T2-weighted image without fat saturation shows a necrotic mass in the right breast and a normal contralateral breast. *B*, Multiplexed sensitivity-encoding (MUSE) diffusion-weighted image (*b* value, 800 sec/mm^2) in the same slice as *A* depicting region of interest (ROI) positioning for quality parameters. *C*, *D*, Apparent diffusion coefficient (ADC) color maps derived from multishot MUSE diffusion-weighted imaging shows ROI placement. Note the ROI placement within the "darkest" part of the solid component of this necrotic mass in, *C*. The ROI of the healthy fibroglandular tissue is delineated in, *D*. The color bar in, *C*, and, *D*, indicates the ADC value range in × 10^{-6} mm^2/sec. ADC values obtained from the ROI in, *B*: mean, 912.8 × 10^{-6} mm^2/sec; minimum, 92 × 10^{-6} mm^2/sec; maximum, 1846 × 10^{-6} mm^2/sec; ROI area, 59.37 mm^2. The ROI values in, *C*: mean, 2043 × 10^{-6} mm^2/sec; minimum, 1133 × 10^{-6} mm^2/sec; maximum, 2868 × 10^{-6} mm^2/sec; ROI area, 52.5 mm^2.

The lesions were identified on contrast-enhanced images, and the slice location was recorded to match diffusion-weighted images at a *b* value of 800 sec/mm^2 for both single-shot DWI and MUSE DWI using the OsiriX viewer. The qualitative parameters were evaluated using a numeric scale for each item: adequate fat suppression (1, failure in suppression; 2, regional fat-water failures but still interpretable; 3, minimal failures in image periphery; 4, perfect fat-water separation), presence of artifact or artifacts (1, nondiagnostic; 2, artifacts but diagnostic; 3, no artifact), lesion visibility (1, yes; 2, no), and image quality (1, better quality than single-shot DWI; 2, same quality as single-shot DWI; 3, worse quality than single-shot DWI), based on the definition of the margins for each lesion. Interreader agreement was calculated for the two readers.

Region of interest selection and quantitative parameters for the comparison of single-shot DWI and MUSE DWI.— Analysis of quantitative parameters was performed using the Advantage Workstation and the aforementioned OsiriX software. All regions of interest were manually drawn by a radiologist (I.D.N.) on the area with the lowest ADC values of the enhancing lesions (mean, 50 mm^2 ± 10). Thereafter, the mean, maximum, and minimum ADC (ADC_{mean}, ADC_{max}, and ADC_{min}, respectively) were recorded in the same slice for both the lesion and fibroglandular tissue in the contralateral healthy breast. SNR for lesion and fibroglandular tissue, as well as contrast-to-noise ratio (CNR), were calculated for each of the 31 lesions (17). Region of interest size was 1 cm^2 for the lesion and for the fibroglandular tissue, which was placed in the healthy contralateral breast within the same slice of the lesion (Fig 2).

Statistical Analysis

Interreader agreement and differences for the qualitative parameters evaluated with single-shot DWI and MUSE DWI were assessed using the Cohen κ coefficient. Differences in quantitative values between phantoms and participants for single-shot DWI and MUSE DWI and tumor differentiation were assessed using the Mann-Whitney *U* test. Statistical software (SPSS for IBM, version 24.0; SPSS, Chicago, Ill) was used for the statistical analysis. $P < .05$ was considered indicative of a significant difference.

Results

MUSE DWI Protocol Optimization on Breast Phantoms

To determine an optimal MUSE DWI protocol, a total of six protocols (protocols A–F, described in Table E2 [supplement]) were tested with varying parameters (number of shots, total acceleration, and time of scan). Protocols D through F had the best overall image quality. Protocol D was selected as the best protocol, enabling good image quality within a clini-

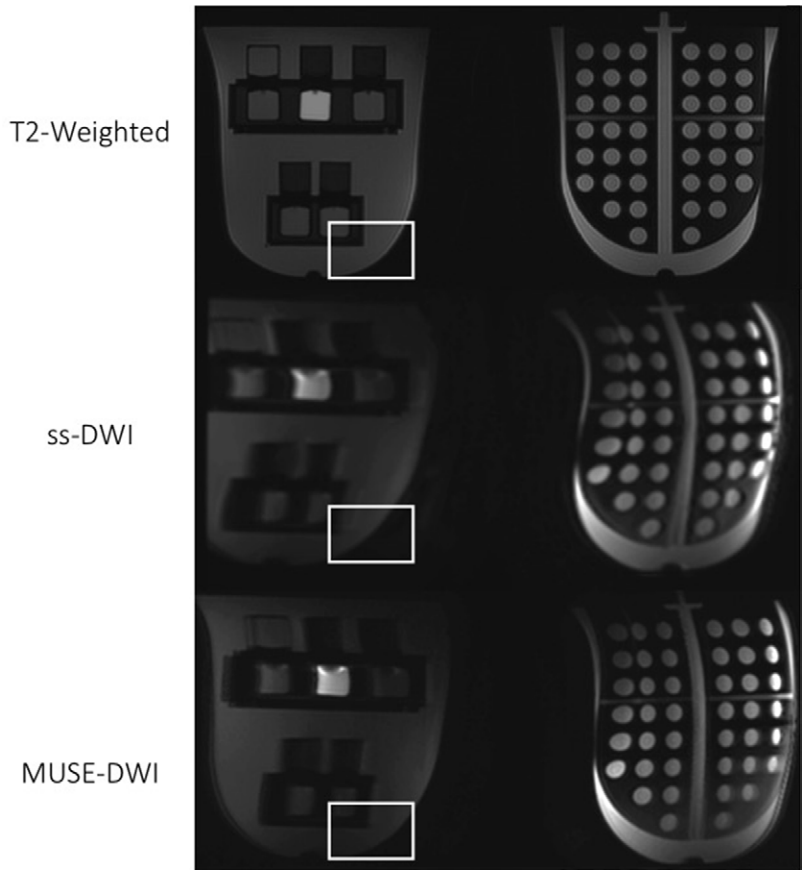

Figure 3: Axial images from phantom testing. T2-weighted image (top panel), single-shot diffusion-weighted image (ss-DWI) (middle panel), and high-spatial-resolution multiplexed sensitivity-encoding diffusion weighted image (MUSE-DWI) with protocol D (bottom panel) are shown. The region of interest is placed to show the presence of geometric distortion artifact on diffusion-weighted images, which is partially corrected with MUSE DWI.

Table 2: Reader Results for Lesion Visibility and Overall Image Quality

Characteristic	Reader 1		Reader 2		Single-Shot DWI	MUSE DWI
Lesion visibility*						
Yes	31	31	30	31	…	…
No	6	6	7	6	…	…
Interreader agreement	…	…	…	…	0.92	0.90
Overall quality of image						
3-Worse quality than single-shot DWI	4		7		…	
2-Same quality	7		6		…	
1-Better quality than single-shot DWI	20		18		…	
Total no. of lesions assessed	31		31		…	
Interreader agreement	…		…		0.70	

Note.—DWI = diffusion-weighted imaging, MUSE = multiplexed sensitivity-encoding.
* Acquisition of 34 axial slices was necessary to cover the entire breast.

cally feasible acquisition time and with reduced distortions compared with single-shot DWI (Table E2 [supplement]) (Fig 3). MUSE DWI protocol D and single-shot DWI were both performed on breast phantoms. The mean SNR values were 460.2 ± 193.9 for MUSE DWI and 200.2 ± 73.5 for single-shot DWI (P = .001). Additionally, no significant differences in ADC values were found for this protocol compared with single-shot DWI (P = .13). Mean ADC values were 1.64 × 10^{-3} mm^2/sec ± 0.01 for MUSE DWI and 1.63 × 10^{-3} mm^2/sec ± 0.058 for single-shot DWI.

MUSE DWI Performs Better than Single-Shot DWI for Breast Lesion Visualization for Qualitative Parameters

Imaging using MUSE DWI (protocol D) and single-shot DWI was performed on the 37 mass lesions. Two radiologists (I.D.N., R.L.G.) compared MUSE DWI and single-shot diffusion-weighted images for their image quality and then assessed fat suppression, artifacts, and lesion visibility for all MUSE DWI and single-shot diffusion-weighted images. The qualitative assessment results, as well as the interreader agreement for each qualitative parameter, are shown in Table 2 and Figure 4. In regard to lesion visibility, six lesions were not visualized with either MUSE DWI or single-shot DWI (31 visible cases). In one case, the lesion was included in the slice gap on diffusion-weighted images, whereas in the remaining five cases insufficient image quality made the lesion undetectable with both techniques. Readers rated MUSE diffusion-weighted images as having better overall quality compared with single-shot diffusion-weighted images in 20 and 18 (κ= 0.70) out of 31 cases. In regard to fat suppression, most of the MUSE DWI cases showed better fat suppression compared with single-shot DWI cases (Fig 4). Only four MUSE DWI cases failed in fat suppression, two of them in more than 75% of the breast. Ghosting and distortion were the main artifacts found with both techniques. Fewer artifacts were detected with MUSE DWI, although among the cases with artifacts, two were considered nondiagnostic. Representative images obtained with MUSE DWI and single-shot DWI in patients with benign and malignant lesions, respectively, are shown in Figures 5 and 6.

MUSE DWI Yields Higher Quality Images of Breast Lesions than Does Single-Shot DWI

To assess the performance of MUSE DWI, we measured SNR, CNR, lesion ADC values, and

fibroglandular ADC values from both MUSE DWI and single-shot diffusion-weighted images. MUSE DWI outperformed single-shot DWI for all quantitative image quality parameters. Lesion SNR was 602.4 ± 393.4 for MUSE DWI and 357.1 ± 264.8 for single-shot DWI (P = .009). Fibroglandular tissue SNR was 314.6 ± 247.1 for MUSE DWI and 205.7 ± 155.7 for single-shot DWI (P = .05). CNR was 330.8 ± 282 for MUSE DWI and 151.3 ± 155.8 for single-shot DWI (P = .008).

We next assessed ADC values from acquired breast images. Representative images of MUSE DWI and single-shot DWI and their corresponding ADC maps from patients with benign and malignant lesions are shown in Figure 7. Lesion ADC values showed no significant differences between MUSE DWI and single-shot DWI (P = .96, P = .28, and P = .49 for ADC_{mean}, ADC_{max}, and ADC_{min}, respectively) (Table 3).

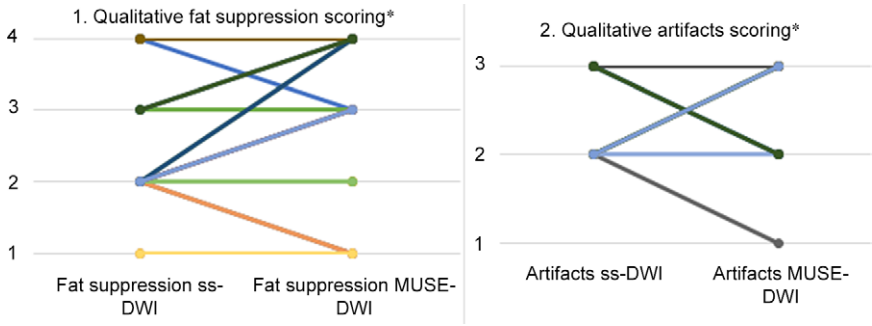

Figure 4: Plot 1 shows the improvement in fat suppression for multishot multiplexed sensitivity-encoding diffusion-weighted imaging (MUSE-DWI) compared with single-shot DWI (ss-DWI) in 37 patients for reader 1. The numbers on the y-axis represent categories as follows: 1, failure in suppression; 2, regional fat-water failures but still interpretable; 3, minimal failures in image periphery; 4, perfect fat-water separation. In nine cases, MUSE DWI improved fat suppression; MUSE DWI performed worse than single-shot DWI in only three cases. This represents a 21% increase in fat suppression quality. Similar findings were found with reader 2. Plot 2 shows an improvement of 5% in image artifacts for MUSE DWI compared with single-shot DWI in 37 patients for reader 1. The numbers in the y-axis represent categories as follows: 1, nondiagnostic; 2, artifacts but diagnostic; 3, no artifacts. In six cases, MUSE DWI presented fewer artifacts. Reader 2 did not find an improvement compared with reader 1. * = numbers shown of a total of 37 breast lesions assessed.

Next, we found that fibroglandular tissue ADC values, ADC_{mean} and ADC_{min}, were not significantly different for MUSE DWI and single-shot DWI (P = .81 and P = .19, respectively). For MUSE DWI, average ADC_{mean} was 1.6×10^{-3} mm²/sec ± 0.33 and average ADC_{min} was 0.82×10^{-3} mm²/sec ± 0.41. For single-shot DWI, average ADC_{mean} was 1.59×10^{-3} mm²/sec ± 0.28 and average ADC_{min} was 0.94×10^{-3} mm²/sec ± 0.42. Significant differences were found in ADC_{max} values (P = .03) when comparing MUSE DWI (2.35×10^{-3} mm²/sec ± 0.56) and single-shot DWI (2.12×10^{-3} mm²/sec ± 0.38). Values for ADC, SNR, and CNR are summarized in Table 3.

When using MUSE DWI for lesion differentiation in a subgroup of 28 lesions with histopathology or follow-up, ADC_{mean} was significantly different between malignant and benign lesions (P < .001). Average ADC_{mean} value was 1.09×10^{-3} mm²/sec ± 0.12 for malignant lesions and 1.39×10^{-3} mm²/sec ± 0.14 for benign lesions. Taken together, MUSE DWI provides higher breast lesion imaging quality than does single-shot DWI and could additionally be used to differentiate between malignant and benign lesions.

Discussion

We investigated the qualitative and quantitative performance of MUSE DWI in the breast compared with single-shot DWI to allow high spatial resolution and alleviate image distortions. We hypothesized that breast lesions could be visualized with higher image quality using MUSE DWI. Our results demonstrated that MUSE DWI significantly outperformed single-shot DWI for quantitative image quality parameters in phantoms and participants. ADC values from MUSE DWI did not differ from those of single-shot DWI; thus, MUSE DWI can differentiate malignant lesions from benign lesions with a significant difference. MUSE DWI improved image quality (ie, enhanced lesion conspicuity) with a substantial interreader agreement in the visual qualitative analysis.

MUSE DWI was designed to minimize artifacts by incorporating the sensitivity-encoding conventional parallel imaging technique to correct random motion-induced phase variations across echo-planar imaging segments (13). Compared with sensitivity encoding alone, MUSE DWI has a better SNR, given its improved matrix inversion conditioning, and has shown high spatial resolution in previous investigations (13,18,19). MUSE DWI has also been extended to account for macroscopic pixel misregistration as well as motion-induced phase errors in a technique called augmented MUSE DWI (20). In accordance with these previous investigations, our preliminary study in the breast found that the quality of the image with MUSE DWI was ostensibly better, resulting in improved lesion delineation compared with single-shot DWI. Additionally, MUSE DWI achieved reasonably improved fat suppression and showed better artifact correction compared with single-shot DWI in the qualitative assessment of the images from patients. This is clinically relevant, since DWI distortions around areas of field inhomogeneity are problematic (eg, around the nipple or inframammary crease). Two MUSE DWI cases with artifacts resulted in nondiagnostic images according to the subjective evaluation of one of the readers in our study. This may be related to the fact that MUSE DWI was performed at the end of the scan in all cases, during which motion is more likely to occur due to patient discomfort. Although there were no differences in fat suppression acquisition parameters between the two sequences, readers agreed in a better perceived fat suppression, which may be due to an improved overall image quality.

Currently, the diagnostic DWI clinical protocol in our institution uses a 3.9-mm slice thickness with four averages as the standard of care. The slice thickness limitation was from the spatial spectral water selective excitation pulse for better fat suppression. We can further increase the spatial resolution or reduce the slice thickness based on available gradient systems

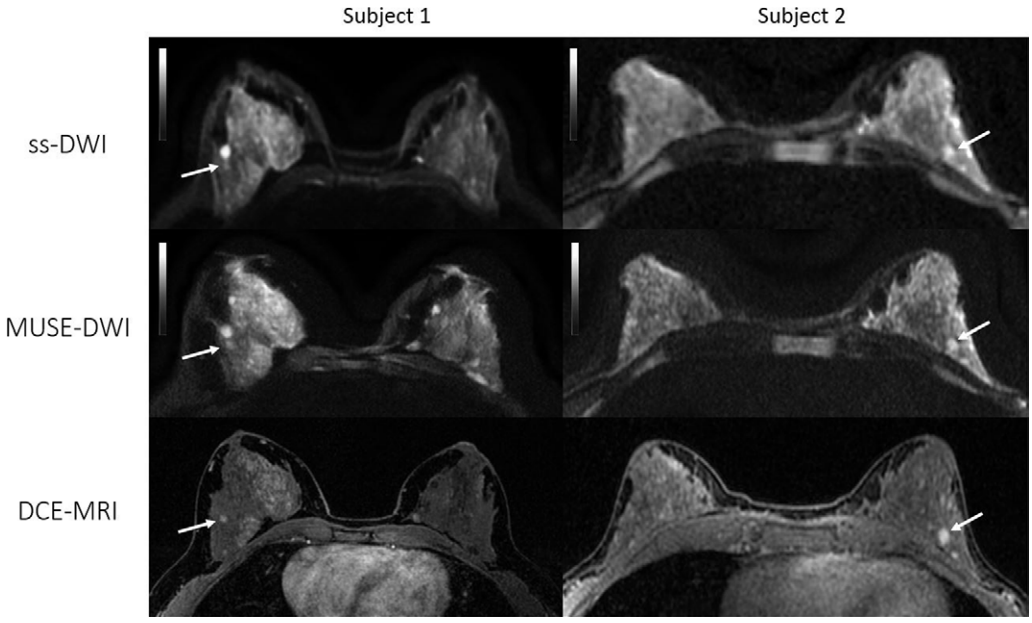

Figure 5: Axial images from two patients with benign lesions. Left: Patient 1, a 43-year-old woman with a 5-mm enhancing focus in the outer right breast in which stability was verified after 2-year follow-up (arrow). Right: Patient 2, a 47-year-old woman with an enhancing 7-mm nodule in the lower inner left quadrant (arrow). Biopsy results revealed fibroadenoma. Multiplexed sensitivity-encoding diffusion-weighted imaging (MUSE-DWI) yielded a sharper delineation of the breast parenchyma, and lesion contours appear to be more defined than in single-shot DWI (*b* value, 800 sec/mm^2) (ss-DWI). These two examples were categorized as 1 (better overall image quality with MUSE DWI than with single-shot DWI) by both readers. DCE-MRI = dynamic contrast-enhanced MRI.

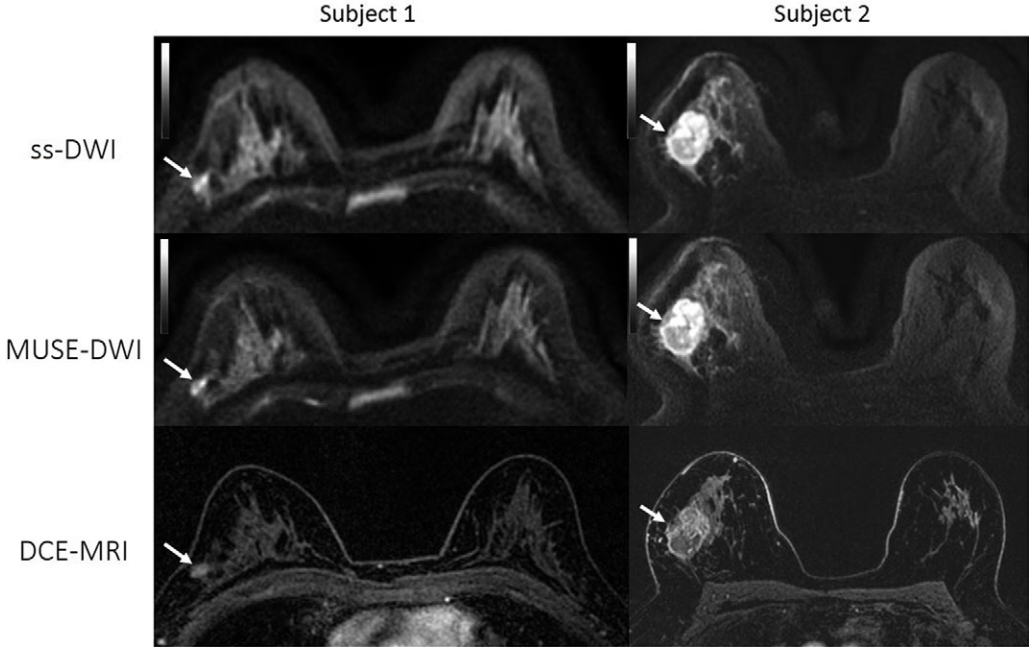

Figure 6: Axial images from two patients with biopsy-proven invasive ductal carcinoma. Left: Patient 1, a 36-year-old woman with a 9-mm mass in the upper outer quadrant of the right breast (arrow). Right: Patient 2, a 57-year-old woman with a 36-mm necrotic mass in the right upper breast (arrow). Both readers assigned category 1 (better overall image quality with multishot multiplexed sensitivity-encoding diffusion-weighted imaging [MUSE-DWI] than with single-shot DWI [ss-DWI]) for overall image quality since MUSE DWI (*b* value, 800 sec/mm^2) showed better lesion delineation compared with single-shot DWI (*b* value, 800 sec/mm^2). Note also that artifact seen with single-shot DWI is partially corrected at MUSE DWI in patient 1.

within different clinical scanners. In this study, we selected the same slice thickness and averages with MUSE DWI to evaluate the feasibility of the MUSE DWI sequence in patients. For a two-shot MUSE acquisition, we would normally expect a doubling in scan time. However, since we observed higher SNR and CNR with minimum artifacts in MUSE DWI, it is

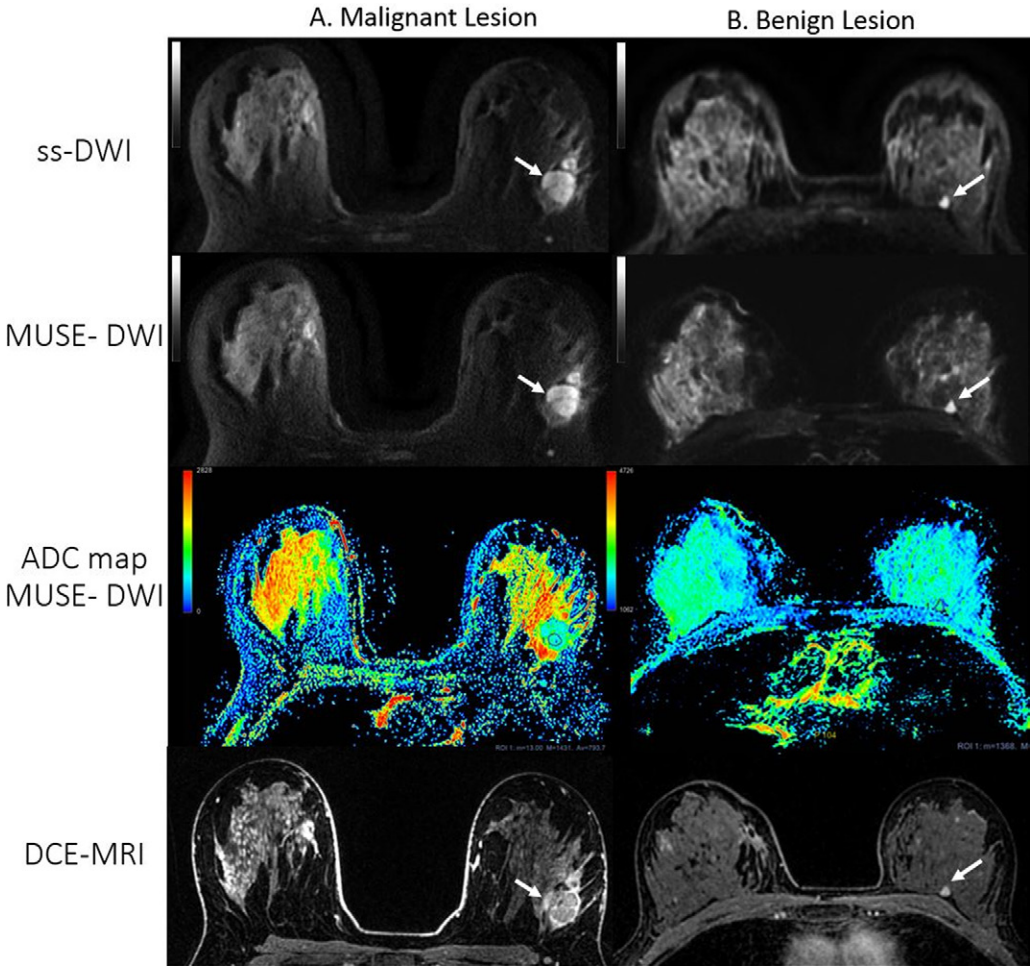

Figure 7: Axial single-shot diffusion-weighted images (ss-DWI), images from multiplexed sensitivity-encoding DWI (MUSE-DWI), apparent diffusion coefficient (ADC) maps, and dynamic contrast-enhanced MRI (DCE-MRI) images from two patients with lesions (white arrows). *A*, Images in a 27-year-old woman with a 25-mm irregular heterogeneously enhancing mass in the left breast. A satellite nodule is evident anterior to the main lesion. At biopsy, the lesion was identified as invasive ductal carcinoma. Readers considered the overall image quality for this case to be worse (category 3) with MUSE DWI than with single-shot DWI. *B*, A 55-year-old woman with a history of right breast cancer after right lumpectomy. A 6-mm enhancing lesion is seen in the posterior third of the left breast (arrow), which was unchanged for the previous 2 years. Both readers scored a better overall image quality (category 1) with MUSE DWI for this case. ADC values are measured in × 10^{-6} mm^2/sec for both images. ADC values obtained from the region of interest (ROI) in, *A*: mean, 793.7 × 10^{-6} mm^2/sec; minimum, 13 × 10^{-6} mm^2/sec; maximum, 1431 × 10^{-6} mm^2/sec; region of interest area, 57.4 mm^2. ADC values obtained from the ROI in, *B*: mean, 2200 × 10^{-6} mm^2/sec; minimum, 1368 × 10^{-6} mm^2/sec; maximum, 2928 × 10^{-6} mm^2/sec; region of interest area, 41.2 mm^2. Blue indicates lower ADC value, red indicates higher ADC value. Note that the minimum ADC threshold value in the color bar for lesion A is 0 ,whereas in the color bar for lesion B it is 1062 to enhance visibility of this benign lesion.

possible to reduce the number of averages to decrease scan time impact while maintaining satisfactory image quality. Additionally, shorter readout duration of MUSE DWI compared with single-shot DWI results in less image blurring and, therefore, an improved resolution.

Because navigator echoes are not necessary for MUSE DWI, the scan time can be reduced. Even faster acquisition times have been described using a three-dimensional multiband MUSE approach in the brain; this approach yielded a high spatial resolution and SNR but unfortunately did not correct motion artifacts properly (21). Other high-spatial-resolution DWI sequences using gradient-echo imaging, such as the double-echo steady-state sequence, have also been investigated for their potential in breast lesion detection with short scan times, fewer artifacts, and reduced distortion relative to single-shot DWI echo-planar imaging (22,23).

Quantitative MUSE DWI ADC values were comparable to those obtained with single-shot DWI. However, further research is needed with multishot DWI in this regard, as Zhang et al (24) showed multishot DWI yielded high-quality images with sufficient reproducibility in ADC values while Deng et al (25) reported that ADC values were greater for multishot DWI with PROPELLER than for single-shot DWI in liver tissues and in phantoms. Previous work using 3-T magnets conducted by Bogner et al (26,27) reported optimal *b* values around 850 sec/mm^2 and an ADC cutoff of 1.25 × 10^{-3} mm^2/sec for lesion differentiation. The ADC values in these studies are in agreement with our results, which are also consistent

Table 3: Results Comparing Mean Values for ADC, SNR, and CNR in Patients

Endpoint and Sequence	Mean	*P* Value
ADC mean lesion ($\times 10^{-3}$ mm^2/sec)		.96
Single-shot DWI	1.28 ± 0.26	…
MUSE DWI	1.28 ± 0.26	…
ADC maximum lesion ($\times 10^{-3}$ mm^2/sec)		.28
Single-shot DWI	1.78 ± 0.39	…
MUSE DWI	1.97 ± 0.58	…
ADC minimum lesion ($\times 10^{-3}$ mm^2/sec)		.49
Single-shot DWI	0.65 ± 0.55	…
MUSE DWI	0.56 ± 0.47	…
ADC mean FGT ($\times 10^{-3}$ mm^2/sec)		.81
Single-shot DWI	1.59 ± 0.28	…
MUSE DWI	1.6 ± 0.33	…
ADC maximum FGT ($\times 10^{-3}$ mm^2/sec)		.03
Single-shot DWI	2.12 ± 0.38	…
MUSE DWI	2.35 ± 0.56	…
ADC minimum FGT ($\times 10^{-3}$ mm^2/sec)		.19
Single-shot DWI	0.94 ± 0.42	…
MUSE DWI	0.82 ± 0.41	…
SNR lesion		.009
Single-shot DWI	357.1 ± 264.8	…
MUSE DWI	602.4 ± 393.4	…
SNR FGT		.054
Single-shot DWI	205.7 ± 155.7	…
MUSE DWI	314.6 ± 247.1	…
CNR		.008
Single-shot DWI	151.3 ± 155.8	…
MUSE DWI	330.8 ± 282	…

Note.—Unless otherwise indicated, data are means ± standard deviations. ADC = apparent diffusion coefficient, CNR = contrast-to-noise ratio, DWI = diffusion-weighted imaging, FGT = fibroglandular tissue, MUSE = multiplexed sensitivity-encoding, SNR = signal-to-noise ratio.

with previously reported ADC values for normal fibroglandular tissue (28).

A limitation of this preliminary study was the relatively small number of patients with small lesions; therefore, the full potential of the high-spatial-resolution MUSE DWI sequence in breast lesion detection has not been explored and will be addressed in future studies. Other groups have investigated the potential of multishot DWI sequences in the breast (27,29,30). A comparison of MUSE DWI with these techniques would be desirable and could be addressed in future studies. Further research is needed to optimize MUSE DWI protocols and to compare this sequence with other multishot DWI sequences to appreciate the full gain of this technique in the breast.

In conclusion, this study demonstrates that high-spatial-resolution MUSE DWI of breast tumors is feasible and can be easily implemented with a routine breast MRI protocol. It significantly outperforms single-shot DWI for breast image quality and is at least as good as the latter in distinguishing malignant and benign lesions.

Acknowledgment: The authors thank Joanne Chin for manuscript editing.

Author contributions: Guarantors of integrity of entire study, I.D.N., T.L., K.P., S.B.T.; study concepts/study design or data acquisition or data analysis/interpretation, all authors; manuscript drafting or manuscript revision for important intellectual content, all authors; approval of final version of submitted manuscript, all authors; agrees to ensure any questions related to the work are appropriately resolved, all authors; literature research, I.D.N., R.L.G., T.L., A.G., K.P., S.B.T.; clinical studies, R.L.G., E.A.M., T.L., K.P., S.B.T.; experimental studies, T.L., M.M.F.; statistical analysis, I.D.N., T.L.; and manuscript editing, all authors

Disclosures of Conflicts of Interest: **I.D.N.** disclosed no relevant relationships. **R.L.G.** disclosed no relevant relationships. **E.A.M.** disclosed no relevant relationships. **T.L.** disclosed no relevant relationships. **M.M.F.** Activities related to the present article: disclosed no relevant relationships. Activities not related to the present article: is and employee of and holds stock in GE Healthcare. Other relationships: disclosed no relevant relationships. **A.G.** Activities related to the present article: disclosed no relevant relationships. Activities not related to the present article: is an employee of GE Healthcare. Other relationships: disclosed no relevant relationships. **K.P.** disclosed no relevant relationships. **S.B.T.** disclosed no relevant relationships.

References

1. Partridge SC, Nissan N, Rahbar H, Kitsch AE, Sigmund EE. Diffusion-weighted breast MRI: clinical applications and emerging techniques. J Magn Reson Imaging 2017;45(2):337–355.
2. Jezzard P, Balaban RS. Correction for geometric distortion in echo planar images from B0 field variations. Magn Reson Med 1995;34(1):65–73.
3. Wu W, Miller KL. Image formation in diffusion MRI: a review of recent technical developments. J Magn Reson Imaging 2017;46(3):646–662.
4. van Pul C, Roos FG, Derksen OS, et al. A comparison study of multishot vs. single-shot DWI-EPI in the neonatal brain: reduced effects of ghosting compared to adults. Magn Reson Imaging 2004;22(9):1169–1180.
5. Madore B, Chiou JY, Chu R, Chao TC, Maier SE. Accelerated multi-shot diffusion imaging. Magn Reson Med 2014;72(2):324–336.
6. Pipe JG, Farthing VG, Forbes KP. Multishot diffusion-weighted FSE using PROPELLER MRI. Magn Reson Med 2002;47(1):42–52.
7. Wang FN, Huang TY, Lin FH, et al. PROPELLER EPI: an MRI technique suitable for diffusion tensor imaging at high field strength with reduced geometric distortions. Magn Reson Med 2005;54(5):1232–1240.
8. Li Z, Pipe JG, Lee CY, Debbins JP, Karis JP, Huo D. X-PROP: a fast and robust diffusion-weighted propeller technique. Magn Reson Med 2011;66(2):341–347.
9. Atkinson D, Porter DA, Hill DL, Calamante F, Connelly A. Sampling and reconstruction effects due to motion in diffusion-weighted interleaved echo planar imaging. Magn Reson Med 2000;44(1):101–109.
10. Bammer R, Stollberger R, Augustin M, et al. Diffusion-weighted imaging with navigated interleaved echo-planar imaging and a conventional gradient system. Radiology 1999;211(3):799–806.
11. Robson MD, Anderson AW, Gore JC. Diffusion-weighted multiple shot echo planar imaging of humans without navigation. Magn Reson Med 1997;38(1):82–88.
12. Hu Y, Levine EG, Tian Q, et al. Motion-robust reconstruction of multishot diffusion-weighted images without phase estimation through locally low-rank regularization. Magn Reson Med 2019;81(2):1181–1190.
13. Chen NK, Guidon A, Chang HC, Song AW. A robust multi-shot scan strategy for high-resolution diffusion weighted MRI enabled by multiplexed sensitivity-encoding (MUSE). Neuroimage 2013;72:41–47.
14. Pruessmann KP, Weiger M, Scheidegger MB, Boesiger P. SENSE: sensitivity encoding for fast MRI. Magn Reson Med 1999;42(5):952–962.
15. King KF. ASSET – parallel imaging on the GE scanner. Presented at the Second International Workshop on Parallel MRI, Zurich, Switzerland, 2004; 15–17.

16. Dietrich O, Raya JG, Reeder SB, Reiser MF, Schoenberg SO. Measurement of signal-to-noise ratios in MR images: influence of multichannel coils, parallel imaging, and reconstruction filters. J Magn Reson Imaging 2007;26(2):375–385.
17. Li X, Huang W, Rooney WD. Signal-to-noise ratio, contrast-to-noise ratio and pharmacokinetic modeling considerations in dynamic contrast-enhanced magnetic resonance imaging. Magn Reson Imaging 2012;30(9):1313–1322.
18. Chang HC, Gaur P, Chou YH, Chu ML, Chen NK. Interleaved EPI based fMRI improved by multiplexed sensitivity encoding (MUSE) and simultaneous multi-band imaging. PLoS One 2014;9(12):e116378.
19. Bammer R, Keeling SL, Augustin M, et al. Improved diffusion-weighted single-shot echo-planar imaging (EPI) in stroke using sensitivity encoding (SENSE). Magn Reson Med 2001;46(3):548–554.
20. Guhaniyogi S, Chu ML, Chang HC, Song AW, Chen NK. Motion immune diffusion imaging using augmented MUSE for high-resolution multi-shot EPI. Magn Reson Med 2016;75(2):639–652.
21. Bruce IP, Chang HC, Petty C, Chen NK, Song AW. 3D-MB-MUSE: a robust 3D multi-slab, multi-band and multi-shot reconstruction approach for ultrahigh resolution diffusion MRI. Neuroimage 2017;159:46–56.
22. Daniel BL, Granlund KL, Moran CJ, et al. Breast MRI without gadolinium: utility of 3D DESS, a new 3D diffusion weighted gradient-echo sequence. Eur J Radiol 2012;81(suppl 1):S24–S26.
23. Granlund KL, Staroswiecki E, Alley MT, Daniel BL, Hargreaves BA. High-resolution, three-dimensional diffusion-weighted breast imaging using DESS. Magn Reson Imaging 2014;32(4):330–341.
24. Zhang Y, Holmes J, Rabanillo I, Guidon A, Wells S, Hernando D. Quantitative diffusion MRI using reduced field-of-view and multi-shot acquisition techniques: validation in phantoms and prostate imaging. Magn Reson Imaging 2018;51:173–181.
25. Deng J, Miller FH, Salem R, Omary RA, Larson AC. Multishot diffusion-weighted PROPELLER magnetic resonance imaging of the abdomen. Invest Radiol 2006;41(10):769–775.
26. Bogner W, Gruber S, Pinker K, et al. Diffusion-weighted MR for differentiation of breast lesions at 3.0 T: how does selection of diffusion protocols affect diagnosis? Radiology 2009;253(2):341–351.
27. Bogner W, Pinker-Domenig K, Bickel H, et al. Readout-segmented echo-planar imaging improves the diagnostic performance of diffusion-weighted MR breast examinations at 3.0 T. Radiology 2012;263(1):64–76.
28. McDonald ES, Schopp JG, Peacock S, et al. Diffusion-weighted MRI: association between patient characteristics and apparent diffusion coefficients of normal breast fibroglandular tissue at 3 T. AJR Am J Roentgenol 2014;202(5):W496–W502.
29. Wisner DJ, Rogers N, Deshpande VS, et al. High-resolution diffusion-weighted imaging for the separation of benign from malignant BI-RADS 4/5 lesions found on breast MRI at 3T. J Magn Reson Imaging 2014;40(3):674–681.
30. Kanao S, Kataoka M, Iima M, et al. High-resolution diffusion-weighted MRI of the breast using readout-segmented EPI and single-shot EPI. Imaging Med 2017;9(6):185–190.